Proceedings of the 3rd Croatian Conference on Earthquake Engineering - 3CroCEE
19–22 March 2025, Split, Croatia

DOI: https://doi.org/10.5592/CO/3CroCEE.2025.145

ANALYSIS OF REINFORCED CONCRETE BEAM-COLUMN JOINT IN ANSYS SOFTWARE

Ivana Drobnjak [(1)], Marina Rakočević [(2)]

[(1)] *Teaching Assistant, University of Montenegro, Faculty of Civil Engineering, ivanadrobnjak25@gmail.com*
[(2)] *Full professor, University of Montenegro, Faculty of Civil Engineering, marinara@ucg.ac.me*

Abstract

In many countries, such as Montenegro, numerous existing reinforced concrete (RC) buildings were designed and built before the adoption of modern seismic codes. These buildings make up a significant portion of Montenegro's RC building stock, making their assessment, retrofitting, and strengthening an urgent research topic. This shortcoming because of insufficient transverse reinforcement, poor energy dissipation, and plastic hinges in critical areas, making shear failures in RC beam-column joints one of the most common structural failure types. Examining and modelling these RC joints and comparing results with experimental data is essential for advancing seismic resilience. The primary goal of this paper was to improve understanding of RC joints, focusing on their vulnerability and critical role in structural integrity. Although these joints represent a local failure point, their breakdown can lead to the collapse of the entire structure. Another aim is to create a foundation for further research, focusing on numerical and experimental analyses of strengthened/retrofitted RC joints.
A nonlinear static analysis of an RC joint was conducted using ANSYS software (version 24.2) with selected material models (CPT215 and REINF264) representing the nonlinear behaviour of concrete and reinforcement, respectively. The load was applied as displacement at the beam end in two steps, with a constant axial force in the column. Vertical force-displacement diagrams were compared with experimental results and those in the ANSYS guide (version 19.1) to verify the convergence and accuracy of results.
Mesh density was varied, using finite elements (FE) of different sizes and shapes, including hexahedral and prismatic forms. Results showed that element size significantly affects numerical accuracy. Additionally, prismatic elements with triangular base achieving faster convergence. The runtime analysis using different mesh densities and finite element types underscored how mesh and element selection impact the balance between modeling accuracy and computational efficiency.

Keywords: Reinforced Concrete joints, Numerical and experimental analysis, Nonlinear static analysis, ANSYS software

Proceedings of the 3rd Croatian Conference on Earthquake Engineering - 3CroCEE
19–22 March 2025, Split, Croatia

DOI: https://doi.org/10.5592/CO/3CroCEE.2025.145

1. Introduction

Many countries did not design reinforced concrete (RC) structures to effectively withstand seismic forces before the 1970s. These structures often exhibit insufficient reinforcement details and inadequate transverse reinforcement, which compromise their lateral strength, energy dissipation capacity, and resistance to plastic hinge formation during earthquakes [1]. In Montenegro, seismic design regulations were first implemented in 1964 after the Skopje earthquake, and today, Eurocodes serve as the sole applicable standards. Common failure mechanisms include shear failure at beam-column joints, column shear failure, and weak-story collapse. RC joints are particularly susceptible to damage, potentially leading to the collapse of the entire structure, as illustrated in Figures 1–3.

Figure 1. Northridge Earthquake, California, 1994, [2]

Figure 2. Izmir Earthquake, Turkey, 1999, [2]

Figure 3. Kocaeli Earthquake, Turkey, 1999, [1]

The "weak column-strong beam" mechanism contradicts the principles of performance-based design, which prioritise ductile joints and follow a "strong column-weak beam" strategy. Allowing beams to lose strength is preferable to column failure, as plastic hinges forming at beam-column connections can compromise the overall stability of the structure, rendering this mechanism inappropriate for design purposes.

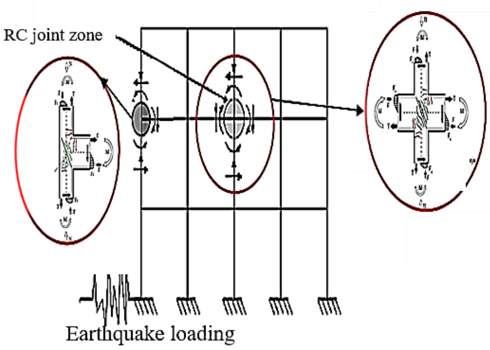

Figure 4. Forces that arise in the beam-column joint zone during an earthquake, [3-4]

In a two-dimensional RC frame exposed to an earthquake, both columns and beams are subjected to shear and bending forces, as shown in Figure 4. Beams primarily endure shear forces and bending moments, while columns must withstand not only these forces but also gravitational loads. Compressive and tensile forces in columns and beams are transmitted through corresponding stresses within the joint.

A widely adopted mechanism for shear transfer in joints is the diagonal strut-and-tie model [5], as illustrated in Figure 5. According to Paulay, Park, and Priestley [5], the strength of the diagonal strut governs the RC joint's capacity before failure. As the shear force at the beam-column connection rises, diagonal cracks develop in the joint core, ultimately causing joint failure due to concrete crushing within the core.

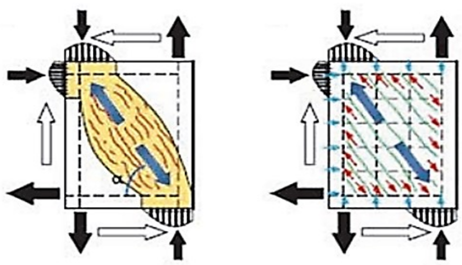

Figure 5. Forces that arise in the beam-column joint zone during an earthquake, [4]

2. Literature review

Since the 1960s, extensive research has been conducted on the behaviour of joints under seismic forces [6]. Hanson and Connor [7] performed some of the earliest experiments, with subsequent advancements reported in [8–11]. Ehsani and Wight [12] investigated the influence of transverse beams, while Pessiki et al. [13] studied joints lacking transverse reinforcement, revealing significant shear cracking upon failure [6]. Tsonos et al. [14] emphasised the effectiveness of inclined overlapping reinforcement in enhancing seismic resistance. An experiment detailed in [15] analysed corner beam-column joints in existing RC structures subjected to low axial pressure to assess their seismic performance.

DOI: https://doi.org/10.5592/CO/3CroCEE.2025.145

The analytical model for RC joints, developed by Park and Paulay [16] and later refined by Paulay et al. [5], identified two primary shear resistance mechanisms under seismic loading. Shear is transferred through a diagonal concrete strut, assuming a perfect bond between concrete and reinforcement. Bond slip occurs when longitudinal reinforcement displaces relative to the concrete due to a loss of bond strength.

The interaction between concrete and reinforcement in joints was examined by Viwathanatepa et al. (1979) [18] and Eligehausen et al. (1983) [19]. While most models assume rigid joints, [20] proposed an alternative approach where the joint core remains elastic during seismic events, even if the surrounding beams and columns sustain damage.

Bracci et al. [21] proposed reducing beam and column stiffness by applying experimentally derived or calculated coefficients. Models that incorporate the behaviour of reinforcement, concrete, and bonding are discussed in [22], while the effects of shear and bond slip are examined in [23, 24]. Shear strength predictions for non-seismically designed joints are provided in [25], and the impact of shear reinforcement is analysed in [26].

Since the 1960s, joint behaviour modelling has advanced significantly, with approaches categorised into plastic hinge models [17, 27–28], component-based models [29–31], and finite element methods (FEM) [3], each offering distinct strengths and limitations.

In software like ETABS and SAP2000, RC structures are modelled with the assumption of rigid beam-column connections. However, this assumption is valid only when failures occur in weaker structural elements rather than in the RC joints themselves [32]. The use of high-strength concrete has reduced column dimensions, increasing the likelihood of joint failures during earthquakes, as observed in Turkey and Taiwan in 1999. Consequently, joints cannot be assumed rigid and are identified as vulnerable structural components, as emphasised in Section 1.

For detailed joint analysis, FEM tools like ANSYS [33] and ABAQUS [34] are widely employed. ABAQUS, extensively used in both engineering practice and academia [35–39], simulates concrete behaviour using damage parameters for compression and tension and models reinforcement with an elastoplastic response to capture steel yielding and failure. The accuracy of such simulations relies heavily on the proper calibration of input parameters against experimental data.

Numerous numerical simulations of RC joints under monotonic loading have been performed [40]. An experimental and numerical study focused on enhancing seismic performance through additional transverse reinforcement in RC joints is presented in [41]. Similarly, [42] provides a numerical analysis in ANSYS of RC joint specimens under cyclic loading to replicate earthquake effects.

3. ANSYS software

3.1. General

In this study, ANSYS software [33] was utilised to simulate the behaviour of RC joints, accurately modelling the properties of both concrete and reinforcement. ANSYS, a leading FEM-based tool, facilitates both static and dynamic analyses for materials that are linear or nonlinear, allowing for the simulation of elastic, inelastic, or viscous behaviours [43]. It enables incremental analysis of stress and strain in RC elements, with capabilities to model large deformations, torsional stress, and contact interaction.

DOI: https://doi.org/10.5592/CO/3CroCEE.2025.145

Model validation was conducted by comparing the results from ANSYS with experimental data to ensure accuracy. The study employed the user-friendly Workbench interface, which is ideal for beginners, while also utilising the APDL scripting language for advanced automation and customization. ANSYS Workbench, Figure 6, supports a wide range of simulations, including structural, thermal, and fluid dynamics analyses. Key features of ANSYS Workbench include an integrated environment (a unified platform for various simulations using ANSYS tools), pre-processing (advanced CAD import and geometry simplification for time efficiency), solution technology (precise simulation of complex phenomena with detailed insights), post-processing (tools for visualising and analysing results through 2D/3D plots, animations, and reports), and model optimisation (optimisation algorithms to enhance performance and reduce costs).

Figure 6. ANSYS Workbench

3.2. Modelling in ANSYS

The general process for conducting any analysis in ANSYS, as shown in Figure 7, whether for simple or complex problems, includes the following steps:

- Pre-processor: Define the geometry, material properties, loads, boundary conditions, and finite element (FE) mesh.
- Analysis: Solve the numerical model defined in the preprocessing phase.
- Post-processor: Analyse and visualise the results.

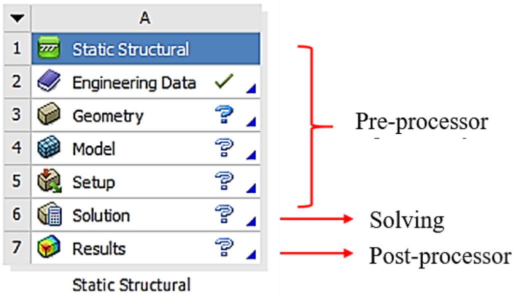

Figure 7. General steps for modelling in ANSYS

Selecting appropriate materials is crucial for modelling and analysing structures, as it significantly impacts the behavior, properties, and durability of the modeled structure or component. ANSYS provides an extensive material library that users can select from and modify as needed. Users can also define and add custom materials with specific properties. The software supports various material types, including linear elastic, isotropic, orthotropic, hyperelastic, viscoelastic, and many other combinations.

In ANSYS, essential material properties include the modulus of elasticity, volumetric density, thermal expansion coefficient, and thermal conductivity. When temperature effects are disregarded, material properties can be treated as linear, requiring only a single iteration. However, properties like the stress-strain relationship are nonlinear and necessitate iterative solutions. Material properties are specified at the element's centre or integration points, depending on the element type [44]. Accurately defining concrete and reinforcement properties in the model module is a critical step for simulating their behaviour and interaction.

In this paper, concrete was modelled using the Coupled Damage-Plasticity (CDP) microplane model, which is well-suited for materials with diverse characteristics. This model accounts for stiffness degradation and material softening, challenges that were previously difficult to simulate, Figure 8.

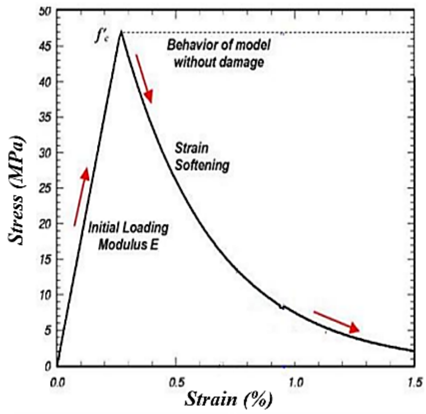

Figure 8. Strain softening effect due to gradual damage of the material

This variant, developed by Zreid in collaboration with ANSYS [45], was designed to incorporate nonlocal interactions, ensuring mesh-independent results. The model represents plasticity using effective stress (in the undamaged space) and employs plastic deformations to capture the resulting damage [45]. Concrete's response under varying stress triaxiality is simulated using the Drucker-Prager function,

Proceedings of the 3rd Croatian Conference on Earthquake Engineering - 3CroCEE
19–22 March 2025, Split, Croatia

DOI: https://doi.org/10.5592/CO/3CroCEE.2025.145

Figure 9. This involves defining the Drucker-Prager yield surface, which considers compressive, tensile, and linear regions.

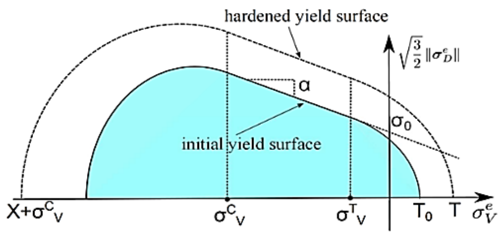

Figure 9. Drucker-Prager function for Microplane model

The initial yield surface defines the boundary of a material's elastic behavior. When the applied stress surpasses this boundary, the hardening process initiates. During this phase, plastic deformations occur, and the elastic region gradually expands until it reaches the hardened yield surface. This new boundary represents the material's updated stress capacity, which will not be exceeded even with further increases in stress. At this stage, material strength decreases, initiating the softening phase, [45]. Defining the CDP microplane model requires specifying 13 parameters, which influence the stress-strain curve, Figure 9.

The concrete material model in ANSYS is implemented using three-dimensional elements (CPT214, CPT215, and CPT216) and two-dimensional elements (CPT211, CPT212, and CPT213). In this study, the CPT215 element was selected, with further details provided in later sections. Reinforcement was modelled using the REINF264 element, with its nonlinear behaviour defined by a bilinear stress-strain isotropic hardening model, which will be explained in more detail subsequently.

To ensure the numerical model accurately represents the physical structure, defining loads and boundary conditions is essential. Loads can include forces applied to faces, edges, or vertices; remote forces or moments applied at distant points; pressures such as fluid, wind, or internal loads; temperature variations; and displacements, commonly used in boundary conditions. Support configurations range from fixed and displacement-defined supports to more advanced options like cylindrical or spherical supports. Proper application of loads and supports is critical to achieving accurate results. Furthermore, generating the finite element mesh is a key step in the simulation process, with ANSYS Workbench offering powerful tools to streamline this task.

Creating the finite element (FE) mesh is a crucial modelling step. ANSYS Workbench provides automated tools with user control over mesh methods, scaling, and edge divisions. This study uses a mesh of hexahedral and prismatic elements with triangular bases to discretize the RC joint, as detailed later.

After preprocessing, ANSYS generates stiffness and mass matrices and load vectors for each element. These are assembled into equations that govern system behavior, solved using methods such as:

- Direct solver: For small to medium models
- Iterative solver: For complex models
- Time integration: For dynamic analyses
- Nonlinear solver: For nonlinear materials or large deformations

If solutions fail to converge, the software adjusts settings or iterations, providing error guidance if needed. Upon successful analysis, users can view results such as displacements, stresses, and deformations through contour plots, animations, graphs, or exported data.

4. Numerical example

This section presents the nonlinear static analysis of an RC exterior joint in ANSYS (version 24.2), validated using experimental data from reference [47] and results from the ANSYS modeling guide (version 19.1), [48]. The paper also investigates how mesh density and element type (hexahedral versus prismatic) influence the speed of solution convergence and the sensitivity of results in nonlinear analysis. Figures 10 - 11 illustrate the geometry of the analysed RC exterior joint [47] and the corresponding geometry model in ANSYS, respectively.

The reinforcement used has the following properties:

Proceedings of the 3rd Croatian Conference on Earthquake Engineering - 3CroCEE
19–22 March 2025, Split, Croatia

DOI: https://doi.org/10.5592/CO/3CroCEE.2025.145

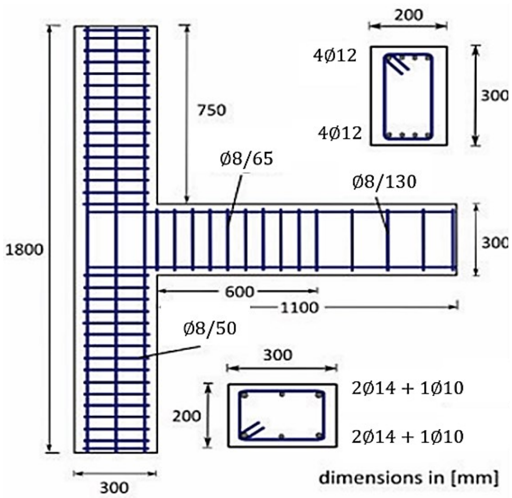

Figure 10. Geometry of the analysed RC joint and reinforcement detailing of the cross sections

$\sigma_y = 470\ MPa$ – yield strength of steel,

The elastic properties of the concrete are:

$f_{uc} = 31.6\ MPa$– compressive strength of concrete,

$\nu = 0.3$ – Poisson's ratio,

$E = 20\ 000\ MPa$ – modulus of elasticity,

$f_{bc} = 36.34\ MPa$ – biaxial strength of concrete

$f_{tc} = 3MPa$ – tensile strength of concrete.

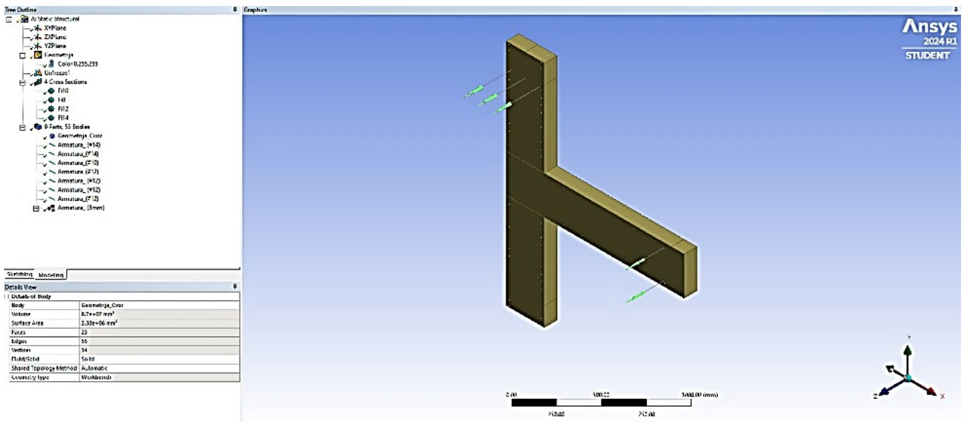

Figure 11. Geometry in ANSYS

Figure 12 shows the APDL commands for defining the CPT215 element and the parameters for the Drucker-Prager model in ANSYS. The REINF264 element from the ANSYS library was used for modelling reinforcement. This element is particularly useful for simulating reinforcement with arbitrary orientations. The nonlinear behavior of reinforcement in the RC joint was defined based on the Bilinear Isotropic Hardening model, as shown in Table 2.

```
!   Commands inserted into this file will be executed just prior to the ANSYS SOLVE command.
!   These commands may supersede command settings set by Workbench.

!   Active UNIT system in Workbench when this object was created:  Metric (mm, kg, N, s, mV, mA)
!   NOTE:  Any data that requires units (such as mass) is assumed to be in the consistent solver unit system.
!                See Solving Units in the help system for more information.


/PREP7
et,matid,CPT215 !define matid to CPT215
KEYOPT,matid,18,2
MP,EX,matid,20000 ! Define Elasticity Modulus (enter a value for E)
MP,NUXY,matid,0.2 ! Define Poisson's ratio
TB,MPLA,matid,,,DPC !Define Drucker-Prager
TBDATA,1,31.6,36.34,3,1,40000,-35 !fuc,fbc,fut,Rt,D,sigVc
TBDATA,7,2,0,2e-5,3000,2000 !R,gamt0,gamc0,betat,betac
TB,MPLA,matid,,,NLOCAL
TBDATA,1,1600,2.5 !nonlocal interaction range c, over nonlocal parameter m

! Replace SOLID185 with CPT215
allsel
esel,s,ename,,SOLID185
emodif,all,type,matid
allsel
! Print out the result:
etlist,all
/SOLU
OUTRES,ALL,ALL
```

Figure 12. APDL commands for defining the CPT215 element and Drucker-Prager parameters

Proceedings of the 3rd Croatian Conference on Earthquake Engineering - 3CroCEE
19–22 March 2025, Split, Croatia

DOI: https://doi.org/10.5592/CO/3CroCEE.2025.145

Table 2. The bilinear isotropic model for steel

The material model for steel - *Bilinear Isotropic Hardening*	
Modulus of elasticity E_s	190 000 MPa
Poisson's ratio, ν_s	0.3
Yield strength, σ_y	470 MPa
Tangent modulus, E_T	1000 MPa

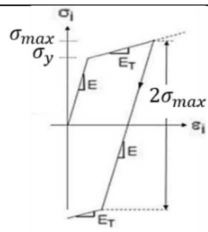

Defining proper boundary conditions is key to accurately modelling the RC joint and replicating rotational supports from the experiment, Figure 13. Load is applied as a constant axial force of 94.80 kN on the column, and an 80 mm displacement at the beam end, Figure 14.

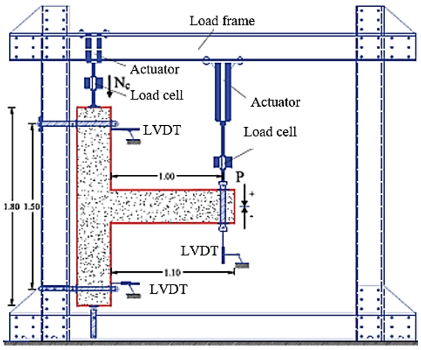

Figure 13. Experiment – analysed specimen with boundary conditions, [48]

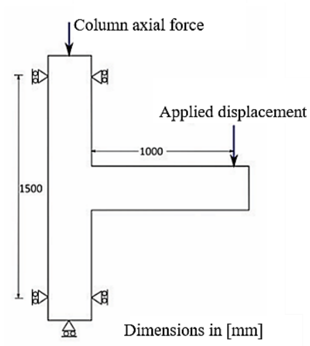

Figure 14. Shematic representation of the model – boundary conditions and loading

Two time steps are considered: $t_1 \in [0,1]$, $t_2 \in [1,2]$, t in seconds. The axial force on the column is applied in time step t_1, and it remains constant at time step t_2. 80 mm displacement is defined in time step t_2.at the beam end.

A finite element (FE) mesh was used to evaluate the accurancy and convergence of numerical solutions. The mesh consisted of hexahedral elements with a size of 25mm, as illustrated in Figure 15.

4.1. Convergence and accurancy of the numerical solutions

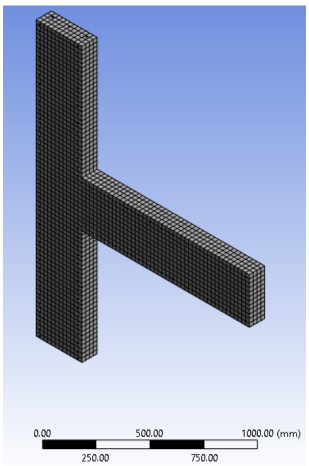

Figure 15. Model discretised with hexahedral finite elements

To verify the convergence and accuracy of the numerical solutions for the RC joint in ANSYS, vertical force–displacement (at the end of the beam) curves were compared with those from the ANSYS guide (version 19.1) and experimental data (Figure 16, Table 3).

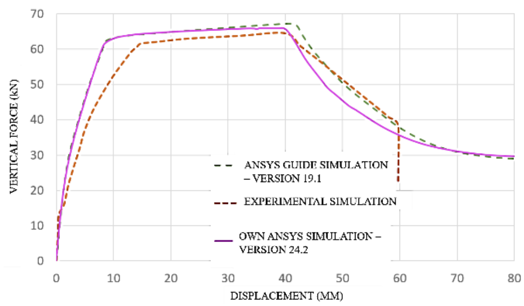

Figure 16. Comparison of vertical force-displacement curves at the end of the beam

The results of the developed model align closely with those from the ANSYS guide, particularly in the curve segment representing elastic behaviour and material hardening. However, material softening in the developed model begins at a displacement of 35 mm, whereas it

Proceedings of the 3rd Croatian Conference on Earthquake Engineering - 3CroCEE
19–22 March 2025, Split, Croatia
Copyright © 2025 CroCEE
DOI: https://doi.org/10.5592/CO/3CroCEE.2025.145

starts at 42 mm in the ANSYS guide model. Beyond this point, as displacement increases, the results converge, with a final discrepancy of 3.51% observed at an 80 mm displacement.

The results in Table 3 are displayed as whole numbers, reflecting the original data format. To maintain consistency, the developed model's results have also been presented in this manner.

An investigation into discrepancies between ANSYS versions 19.1 and 24.2 revealed that variations may arise from differences in operating systems, processor cores, and software configurations. Additional factors include the lack of specific details regarding the ANSYS guide model's load distribution and incremental application. Furthermore, the tolerance value used in the Newton-Raphson method significantly affects numerical accuracy—lower tolerances require more iterations, while higher tolerances increase the risk of errors if convergence is not achieved.

Table 3.

a) Comparison of results obtained from the ANSYS guide with results from the own model

ANSYS GUIDE SIMULATION – VERSION 19.1		OWN ANSYS SIMULATION – VERSION 24.2		DIFFERENCE (%)
DISPLACEMENT (MM)	FORCE (kN)	DISPLACEMENT (MM)	FORCE (kN)	
0	0	0	0	0
1	10	1	11	10.18
1	20	1	18	12.11
2	30	2	29	4.50
4	40	4	40	0.15
6	50	6	47	6.59
8	60	8	61	2.36
8	62	8	61	1.02
9	63	9	62	1.35
12	64	12	64	0.07
20	65	20	65	0.13
35	67	35	66	1.16
40	67	40	66	1.84
42	67	42	62	8.19
42	66	42	62	6.84
43	64	43	60	6.46
45	60	45	53	13.70
46	57	46	51	11.88
49	51	49	47	9.56
52	47	52	43	10.70
57	42	57	38	9.43
60	38	60	35	7.62
63	35	63	34	2.33
67	32	67	32	1.15
71	30	71	31	1.11
76	29	76	30	2.26
80	29	80	30	3.51

b) Comparison of results obtained from the own model with results from experiment

EXPERIMENT		OWN ANSYS SIMULATION – VERSION 24.2		DIFFERENCE (%)
DISPLACEMENT (MM)	FORCE (kN)	DISPLACEMENT (MM)	FORCE (kN)	
0	0	0	0	0.00
0	0	0	0	0.00
0	13	0	11	18.92
1	16	1	18	10.32
2	21	2	29	25.98
3	27	3	36	24.23
4	32	4	40	19.63
5	36	5	45	19.45
6	42	6	47	10.88
8	46	8	61	24.01
10	53	10	63	16.50
13	59	13	64	7.59
14	61	14	64	5.41
15	62	15	64	3.67
17	62	17	65	4.51
23	63	23	65	2.92
32	64	32	66	3.22
40	65	40	66	2.16
43	61	43	60	1.36
46	57	46	51	10.79
49	53	49	47	12.52
53	48	53	42	14.31
56	44	56	39	11.69
58	41	58	37	10.20
60	38	60	35	9.74
60	22	60	35	35.98

The force-displacement curve from the developed ANSYS model closely matches the experimentally obtained curve in terms of shape. However, the most significant deviations occur during the material softening phase. Additionally, it is important to note that experimental results may be influenced by both instrumental and random errors.

4.2. Variation in Finite Element mesh density and type

The finite element (FE) mesh density was initially formed using hexahedral elements, followed by prismatic elements, and the resulting data was analysed and compared. Meshes with element sizes of 35 mm, 50 mm, and 100 mm were generated, as shown in Figure 17, and evaluated against a 25 mm mesh, which served as the benchmark for accuracy and convergence. This methodology was employed to assess the sensitivity of nonlinear numerical analysis results to changes in FE mesh density and to determine the impact of mesh refinement on the accuracy of the results.

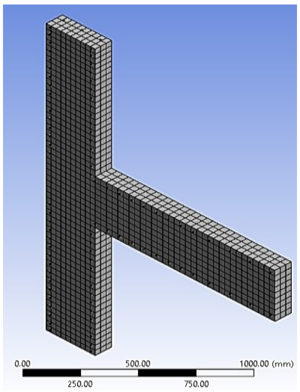

Figure 17. a) Discretisation of the RC joint using finite elements of size 35 mm

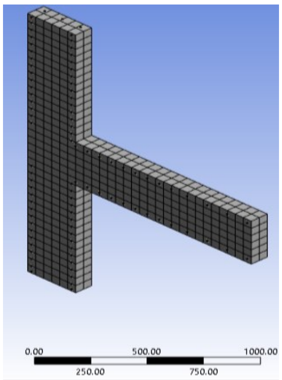

Figure 17. b) Discretisation of the RC joint using finite elements of size 50 mm

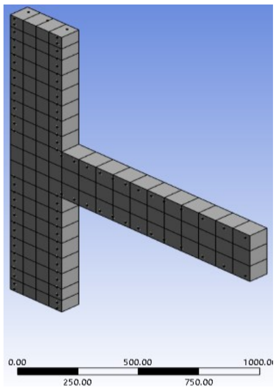

Figure 17. c) Discretisation of the RC joint using finite elements of size 100 mm

DOI: https://doi.org/10.5592/CO/3CroCEE.2025.145

The next section presents the force-displacement curves for models created using different finite element (FE) sizes in the mesh generation process, as illustrated in Figure 18. The size of the finite elements has a significant influence on mesh generation and the accuracy of results, particularly in nonlinear analyses. While variations in FE mesh density have little effect during the elastic phase, discrepancies become more pronounced in later stages. As shown in Figure 18, meshes with element sizes of 100 mm and 50 mm fail to deliver satisfactory results, whereas the 35 mm mesh closely approaches the accuracy of the 25 mm mesh. Smaller elements enhance precision but require longer simulation times and better computational resources.

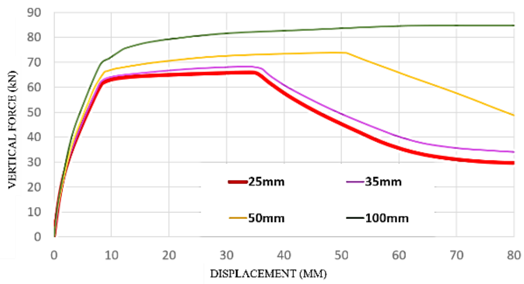

Figure 18. Curve vertical force-displacement at the end of the beam relative to the variation in finite element size

In addition to the element size comparison, the study also evaluated results obtained using hexahedral element meshes alongside models generated with prismatic elements with triangular bases. The prismatic element meshes were created with the same element sizes—35mm, 50mm, and 100mm—as in the previous analysis, Figure 19.

Figure 20 presents a comparison of the vertical force-displacement curves for both types of finite elements used to discretize the analysed RC joint.

It is evident that models with meshes generated using prismatic elements with triangular bases demonstrate faster convergence compared to those with hexahedral elements, particularly for cases involving 35mm element sizes.

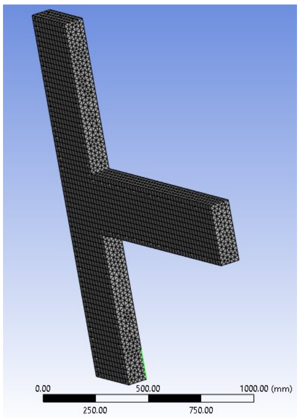
Figure 19. a) Discretisation of the RC joint using prismatic finite elements of size 35 mm

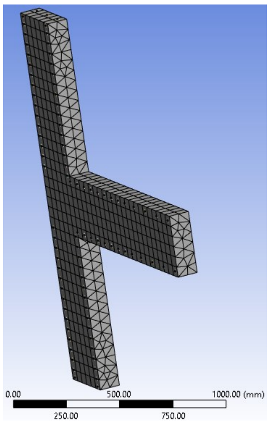
Figure 19. b) Discretisation of the RC joint using prismatic finite elements of size 50 mm

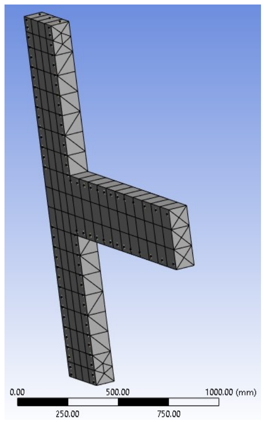
Figure 19. c) Discretisation of the RC joint using prismatic finite elements of size 100 mm

DOI: https://doi.org/10.5592/CO/3CroCEE.2025.145

5. Conclusion

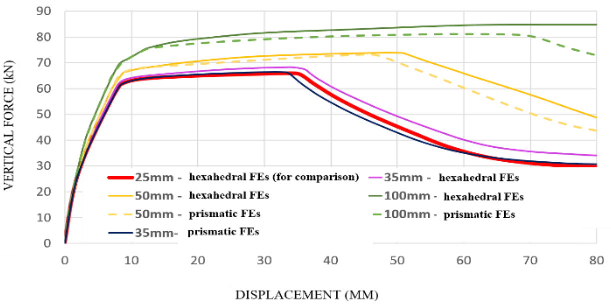

Figure 20 Curve vertical force-displacement at the end of the beam relative to the variation in finite element type

This study conducted a nonlinear static analysis of a reinforced concrete (RC) joint using ANSYS software (version 24.2) to better understand RC joint behaviour and evaluate the feasibility of such connections. It also aimed to provide a foundation for future research involving numerical and experimental analysis of strengthened RC joints. Nonlinear behaviour was modelled using ANSYS material models (CPT215 and REINF264), with loads applied in two steps: displacement at the beam's end and a constant axial force on the column.

Force-displacement curves from the numerical model were compared with experimental data and results from the ANSYS guide (version 19.1) to validate convergence and accuracy. The force-displacement curve generated by own ANSYS model closely aligns in shape with the experimentally obtained curve. However, the most notable discrepancies are observed during the material softening phase. It is also essential to consider that experimental results may be affected by both random and instrumental errors.

Analysis of finite element (FE) mesh density, element size, and type (hexahedral versus prismatic elements with triangular bases) revealed that even for simple geometries, element size has a significant impact on numerical accuracy. Additionally, prismatic elements with triangular bases achieved faster convergence compared to hexahedral elements.

Future research could focus on analysing RC joints under various loading conditions, exploring alternative material models or input parameters, and modelling strengthening techniques for these connections. This would enhance understanding of the factors influencing joint behaviour and performance, contributing to improved design and strengthening of RC structures.

References

[1] Sharbatdar, K., Fakharifar, M. (2009): The Finite Element analysis of RC joints strengthened with external FRP composites, *3rd International Conference on Concrete & Development,* Iran

[2] Hassan, W.M., Park, S., Lopez, R. R., Mosalam, K.M., Moehle, J. P. (2010): Seismic response of older-type reinforced concrete corner, *Proceedings of the 9th U.S. National and 10th Canadian Conference on Earthquake Engineering, Toronto,* Canada

[3] Pan, Z. (2016): Modeling of interior beam-column joints for nonlinear analysis of reinforced concrete frames, *Master thesis, University of Toronto, Department of Civil Engineering*

[4] Coşgun, C. (2013): Retrofit of 3D Reinforced Concrete Beam-Column Joint with FRP, *PhD thesis, Istanbul Technical University, Institute of Science and Technology*

[5] Paulay, T., Park,, R., Priestley, M.J.N. (1978): Reinforced Concrete Beam-Column Joints under Seismic Actions, *ACI Structural Journal 75*

[6] Coşgun, T. et al (2019).: Ispitivanja rubnih spojeva greda-stup postojećih AB konstrukcija na djelovanje potresa, *Časopis Građevinar*, broj 71

[7] Hanson, N.W., Connor, H.W. (1967): Seismic Resistance of Reinforced Concrete Beam- Column Joints, *Journal of the Structural Division - ASCE, 93*

[8] Zhang, L., Jirsa, J.O. (1982): A study of shear behavior of reinforced concrete beam– column joints, *PMFSEL Report 82–1, University of Texas*, Austin, USA

[9] Sarsam ,K.F., Phipps, M.E. (1985): The shear design of in situ reinforced concrete beam– column joints subjected to monotonic loading, *Magazine of Concrete Research, no. 37*

DOI: https://doi.org/10.5592/CO/3CroCEE.2025.145

[10] Pantazopoulou, S., Bonacci, J. (1992): Consideration of questions about beam–column joints, *Aci Structural Journal, 89*

[11] Hwang, J., Lee, H.J. (1999): Analytical model for predicting shear strengths of exterior reinforced concrete beam–column joints for seismic resistance, *Aci Structural Journal 96*

[12] Ehsani, M.R., Wight, J.K. (1986): Effect of beams and slab on behavior of reinforced concrete beam-to-column connections, *Aci Structural Journal, 82*

[13] Pessiki, S.P., Conley, C.H., Gergely,, P., White, R.N. (1990): Seismic behavior of lightly reinforced- concrete column and beam-column joint details, *Technical Report NCEER- 90-0014, National Centre for Earthquake Engineering Research*

[14] Tsonos,, A.G., Tegos, I.A., Penelis, G. (1992): Seismic resistance of type 2 exterior beamcolumn joints reinforced with inclined bars, *Aci Structural Journal, 89*

[15] Higazy, E.M.M., Elnashai,, A.S., Agbabin, M.S. (1996): Behavior of beam column connections under axial column tension, *Journal of Structural Engineering*

[16] Park, R., Paulay, T. (1975): *Reinforced concrete structures*. John Wiley & Sons, Inc., Newyork

[17] Altoontash, A. (2004): Simulation and Damage Models for Performance Assessment of Reinforced Concrete BeamColumn Joints." P*hD Thesis, Department of Civil and Environmental Engineering, Stanford University, California,* United States

[18] Viwathanatepa, S., Popov, E.P., and Bertero, V.V. (1979): Effects of Generalized Loadings on Bond of Reinforcing Bars Embedded in Confined Concrete Blocks, *Rep. No. UCB/ERRC-79/22 ERRC, Univ. of California, Berkeley, CA*

[19] Eligehausen, R., Popov, E.P. and Bertero, V.V. (1983): Local bond Stress-Slip Relationship of Deformed Bars under Generalized Excitations, *EERC Report 83/23, University of California*

[20] Pessiki, S.P., Conley, C.H., Gergely, P., White, R.N. (1990): Seismic behavior of lightly reinforced - concrete column and beam-column joint details, *Technical Report NCEER- 90-0014, National Centre for Earthquake Engineering Research*

[21] Bracci, J.M., Reinhom, A.M., Mander, J.B. (1992): Seismic resistance of R/C frame structures designed only for gravity loads, Part III experimental performance and analytical study of structural model, *Technical Report NCEER-92-0029, National Centre for Earthquake Engineering Research*

[22] Fleury, F., Reynouard, J-M., Merabet, O. (2000): Multicomponent model of reinforced concrete joints for cyclic loading, *Journal of mechanical Engineering 10*

[23] Pantazopoulou, S.J., Bonacci, J.F. (1994): On earthquake-resistant reinforced concrete frame connections, *Canadian Journal of Civil Engineering 21*

[24] Elmorsi, M.S.E. (1998): Analytical modeling of reinforced concrete beam column connections for seismic loading, *PhD thesis, McMaster University, Ontario*, Canada

[25] Hegger, J., Sherif A., Roeser W. (2003): Nonseismic design of beam column joints, *ACI Structural Journal 100*

[26] Hwang, S.J., Lee, H.J., Liao, T.F., Wang, K.C., Tsai, H.H. (2005): Role of hoops on shear strength of reinforced concrete beam-column joints, *ACI Structural Journal 102*

[27] Alath, S., Kunnath, S.K. (1995): Modeling Inelastic Shear Deformation in RC Beam-Column Joints, *Proceedings of the 10th Conference, University of Colorado at Boulder*

[28] Shin, M., LaFave, J.M. (2004): Modeling of Cyclic Joint Shear Deformation Contributions in RC Beam-Column Connections to Overall Frame Behavior, *Structural Engineering and Mechanics, 18(5)*

[29] Ghobarah, A., Youssef, M. (2001): Modeling of RC Beam-Column Joints and Structural Walls, *Journal of Earthquake Engineering, 5(1), 91-111*

[30] Lowes, L.N., Alttontash, A.: (2003): Modeling Reinforced Concrete Beam-Column Joints Subjected to Cyclic Loading, *Journal of Structural Engineering 129(12)*

DOI: https://doi.org/10.5592/CO/3CroCEE.2025.145

[31] Mitra, N., Lowes, L.N. (2007): Evaluation, calibration, and verification of a Reinforced Concrete Beam-Column Joint Model., *Journal of Structural Engineering* 133(1)

[32] Aoyama, H., Otani S., Kitayama K. (1988): Design critiria for reinforced concrete interior beam-column connections, *Proceedings of 9th World Conference on Earthquake Engineering,* Tokyo-Kyoto, Japan

[33] ANSYS Workbench Product Release Notes (2005), USA

[34] ABAQUS 6.12 (2012) – Analysis User's Manual, USA

[35] Ellobody, E., Baile C.G. (2008): Behaviour of unbonded posttensioned one-way concrete slabs*", Advance Structural Engineering, Vol. 11, No.* 1

[36] Zhang, H.M., Lu, X.L., Duan, Y.F., Li J.B. (2011): Experimental study and numerical simulation of partially prefabricated laminated composite RC walls", *Advances in Structural Engineering, Vol. 14, No. 5,* 2011

[37] Alemdar, Z.F., Matamoros, A.B., Browning, J. (2013): High resolution modeling of reinforced concrete bridge columns under seismic loading, *ACI Structural Journal, Vol. 110, No. 5*

[38] Henriques, J., Silva, L.S, Valente I.B. (2013): Numerical modeling of composite beam to reinforced concrete wall joints Part I: Calibration of joint component, *Engineering Structures, Vol. 52*

[39] Abbas, A.A., Mohsin, S.M.S. and Cotsovos, D.M. (2014): Seismic response of steel fibre reinforced concrete beam-column joints", *Engineering Structures, Vol. 59*

[40] Patil, S.S., Manekari, S.S. (2013): Analysis of reinforced beam-column joint subjected to monotonic loading", *IJEIT*

[41] Bindhu, K.R., Jaya, K.P. (2012): Strength and Behavior of Exterior Beam Column Joints with Diagonal cross Bracing Bars. *Asian Journal of Civil Engineering (Building and Housing), 11*

[42] Sohailuddin, S. i Shaikh, M.G. (2013): Finite element modelling of reinforced concrete beam – column joint using ANSYS, *IJSCER*

[43] Lazzari, B.M. (2015): Análise por elementos finitos de peças de concreto armado e protendido sob estados planos de tensão, *Dissertação (Mestrado em Engenharia) – Programa de Pós-Graduação em Engenharia Civil, Universidade Federal do Rio Grande do Sul, Porto Alegre*

[44] *ANSYS Mechanical APDL Element Reference* (2010), USA

[45] Zreid, I., Kaliske, M. (2018): A gradient enhanced plasticity–damage microplane model for concrete, *Computational Mechanics*

[46] Pirket, M. (2020): Non-linear seismic analysis of a concrete gravity dam using a microplane material model, *Master's Thesis, Graz University of Technology, Hydraulics and Geotechnical Engineering*

[47] Chalioris, C.E., Favvata, M. J., Karayannis, C.G. (2008): Reinforced concrete beam–column joints with crossed inclined bars under cyclic deformations, *Earthquake Engineering and Structural Dynamics*

[48] ANSYS Documentation, Release 19.1 (2019), *Demonstration guide – reinforced concrete*

[49] https://www.ansys.com/blog/what-is-apdl, Accessed 21st November 2024

[50] Dr. Daylo APDL Commands - https://cutt.ly/IjsHW8c, Accessed 21st November 2024